

Optimization of highly efficient terahertz generation in lithium niobate driven by Ti:sapphire laser pulses with 30 fs pulse duration

Xiaojun Wu (吴晓君)^{1,*}, Shusu Chai (柴姝愫)¹, Jinglong Ma (马景龙)²,
Baolong Zhang (张保龙)², Chenyi Xia (夏晨懿)³, Zhaoji Fang (方兆吉)¹,
Deyin Kong (孔德胤)¹, Jinguang Wang (王进光)^{2,4}, Hao Liu (刘浩)^{2,4},
Changqing Zhu (朱常青)^{2,4}, Xuan Wang (王暄)², Cunjun Ruan (阮存军)¹,
and Yutong Li (李玉同)^{2,4,5}

¹School of Electronic and Information Engineering, Beihang University, Beijing 100191, China

²Beijing National Laboratory for Condensed Matter Physics, Institute of Physics, Chinese Academy of Sciences, Beijing 100190, China

³School of Automation Science and Electrical Engineering, Beihang University, Beijing 100191, China

⁴School of Physical Sciences, University of Chinese Academy of Sciences, Beijing 100049, China

⁵Collaborative Innovation Center of IFSA (CICIFSA), Shanghai Jiao Tong University, Shanghai 200240, China

*Corresponding author: xiaojunwu@buaa.edu.cn

Received January 1, 2018; accepted February 9, 2018; posted online March 26, 2018

We systematically study the optimization of highly efficient terahertz (THz) generation in lithium niobate (LN) crystal pumped by 800 nm laser pulses with 30 fs pulse duration. At room temperature, we obtain a record optical-to-THz energy conversion efficiency of 0.43% by chirping the pump laser pulses. Our method provides a new technique for producing millijoule THz radiation in LN via optical rectification driven by joule-level Ti:sapphire laser systems, which deliver sub-50-fs pulse durations.

OCIS codes: 190.7110, 040.2235, 160.3730.

doi: 10.3788/COL201816.041901.

The terahertz (THz) frequency range (0.1–10 THz) is located between microwave and infrared (IR) light in the electromagnetic spectrum^[1]. Due to the lack of high power, high energy, efficient sources, and sensitive detectors, this field is underdeveloped compared with other frequencies. Thanks to the advanced ultrafast laser technologies, THz science and technology has experienced unprecedented prosperity since the 1990s^[2]. THz time-domain spectroscopy^[3] and imaging^[4] have led THz technology from laboratory research to some practical applications. However, the lack of bright and intense THz sources still greatly hinders the development of this field^[5], especially for nonlinear THz investigations, like condensed matter physics^[6], water sciences^[7], and the THz biology effect^[8].

Conventional high energy THz sources are electron-accelerator-based facilities^[9], which are large and expensive for applications. For intense THz sources in the frequency range of 0.1–10 THz, ultrafast laser-based sources are very promising. For example, large aperture photoconductive antennas can already deliver more than 12.5 μJ THz pulses with 1.6% conversion efficiency^[10,11]. Laser induced air/gas-plasma is also capable of generating 5 μJ THz pulses^[12]. Such intense THz sources have already shown powerful capabilities in THz nonlinear spectroscopy and time-resolved coherent manipulation in solids, liquids, gas, and plasma. The next goal in strong field THz sources is to achieve millijoule (mJ) pulse energy with peak electric fields higher than megavolts (MV)/centimeter (cm)

and peak magnetic fields higher than tesla (T)^[5]. Optical rectification in nonlinear crystals is one of the most promising ways. Recently, 0.9 mJ THz pulses have already been demonstrated in organic crystals pumped by a Cr:Mg₂SiO₄ laser with a THz peak field of more than 42 MV/cm and 14 T^[13]. However, this kind of intense THz source requires specific pumping wavelengths of 1.2–1.5 μm , and the generated central frequencies are always located in a higher frequency range. For some applications like electron acceleration^[14], the THz biology effect^[8], nonlinear THz metamaterials^[15–17], and condensed matter physics^[18,19], intense THz sources with lower frequencies in 0.1–2.0 THz range are also very important.

The tilted pulse fronts (TPF) technique in lithium niobate (LN) is one of the best candidates for intense THz generation^[20] with lower frequencies. Some nonlinear crystals like LN^[21], GaAs^[22], and ZnTe^[23] have been used for TPF phase matching. MgO-doped LN has the advantages of large nonlinear coefficient, high damage threshold, and large size. Combined with the TPF technique, LN is applicable for all pumping wavelengths. Since this method was demonstrated in 2002, lots of laser systems with the pumping wavelengths covering from 800 nm to 2.0 μm have been employed to generate high energy, strong field THz pulses. Early principle verifications were carried out on commercial Ti:sapphire laser systems with relatively low THz pulse energy yields of several microjoules^[24]. With the further improvement of the TPF

theory^[25], extremely high efficiencies of more than several percent could be obtained with appropriate pumping laser parameters. For example, employing a longer pulse duration of ~ 650 fs at $1.0 \mu\text{m}$ pump wavelength, Huang *et al.* have demonstrated 3.8% optical-to-THz energy conversion efficiency in LN at low temperatures^[26]. Fülöp *et al.* obtained 0.4 mJ THz energy with 70 mJ pumping laser pulses at $1.0 \mu\text{m}$ excitation wavelength^[27]. It is straightforward that the efficiency should be proportional to pump intensity. However, the nonlinear distortion effect hinders the scaling up of the efficiency as well as THz output energy. This effect becomes even more pronounced if sub-50-fs short laser pump pulses are used.

Short pump pulses have a very broad spectrum. After diffraction from a grating in the TPF setup, the diffracted pump beam has a large divergence angle, requiring large optical elements for imaging all the spectrum components into the LN crystal for phase matching^[28]. The large curvature effect combined with chromatic aberration makes the THz generation less efficient. The inherent imperfection of TPF could be magnified for sub-50-fs pump laser pulses. Ultra-short pump pulses have short effective interaction length for THz generation and also introduces free-carrier absorption for THz waves due to high peak intensities^[29]. Free-carrier absorption becomes more pronounced when we employ 800 nm pump pulses rather than $1.0 \mu\text{m}$. In order to avoid damaging the crystal, big pump beams have to be used. As a consequence, only partial pump energy is efficient for THz generation. All these effects are combined inherently in TPF optimization and make the mJ THz generation become a formidable challenge for joule-level (J-level) pump laser pulses with sub-50-fs pulse durations. Previous works are based on the spectrum-cutting method to broaden the pump laser pulses^[30,31]. This method is an effective way for scaling up the THz efficiency, but the output THz energy is relatively low for further applications.

In this work, we systematically investigate the competition effects between the pulse duration and pump energy for efficient THz generation. It is demonstrated that the pulse duration dominates the competition process. A high record optical-to-THz energy conversion efficiency of 0.43% at room temperature is achieved in LN driven by an 800 nm wavelength through stretching pump laser pulses from 30 fs to ~ 187 fs.

A commercial 20 TW Ti:sapphire amplifier (Pulsar 20, Amplitude Systems) is used in our experiment. The laser system consists of a seed, a booster, a stretcher, an amplifier, and a compressor. Inside the seed there is an oscillator producing pulses at 75 MHz repetition rate with 10 fs pulse duration. Laser pulses with 10 Hz repetition rate are picked from 75 MHz by a Pockels cell optical shutter and pre-amplified in the booster. The Offner stretcher is composed of a diffraction grating, a convex mirror, and a concave mirror with eight-pass configuration. An acousto-optics programmable dispersive filter (AOPDF, Dazzler) is used to optimize the pulses or chirp the pulses on purpose. In the following experiments, we use this

AOPDF to chirp the pump laser pulses, therefore varying the pulse duration with positive and negative dispersion. The stretched 800 nm pulses are pumped by a 532 nm green light in the amplifiers and compressed to 30 fs pulse duration. This laser system is capable of providing pump pulse energy up to 500 mJ. The pump beam diameter after the compressor is ~ 40 mm ($1/e^2$). An iris after the compressor is employed to eliminate low-level energy distributed at the outer part of the laser beam, which has no contribution to the THz generation.

The LN-based TPF setup is shown in Fig. 1. The pump laser pulses are diffracted by a grating with 1480 lines/mm line density at a designed incidence angle of 21° . The grating is imaged into the LN crystal by a plano-convex lens with a focal length of 85 mm. The distances of grating-to-lens and lens-to-crystal are ~ 255 mm and ~ 127.5 mm, respectively, implying a demagnification of -0.5 . Therefore, the pump beam on the LN crystal is ~ 20 mm ($1/e^2$) in diameter. A half-wave plate (HWP) is used to rotate the polarization of the pump beam from horizontal to vertical, parallel to the optic axis of the crystal.

The congruent LN crystal is doped with MgO at 6 mol.% and shaped into a triangle prism with 68.1 mm(Y) $_62^\circ_64.0$ mm $_62^\circ_40$ mm (height, z axis), and the entry surface for the IR pump beam (68.1 mm \times 40 mm rectangle) is anti-reflection (AR) coated at 700–1060 nm in order to overcome the Fresnel loss. The THz output surface is AR coated for THz waves by polyimide layers with the thickness of $\sim 100 \mu\text{m}$. In this way, the measured extracted THz energy is $\sim 30\%$ enhanced compared with that without AR coating. The output THz energy is detected by a pyroelectric detector (Gentec-EO, SDX-1152). In front of the

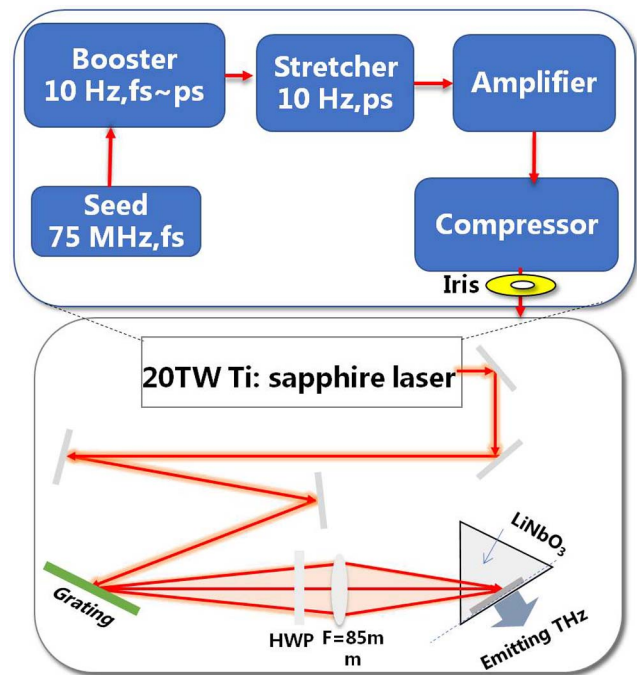


Fig. 1. Schematic of THz generation with the TPF technique.

detector sensor, there is a high resistivity Si wafer to block the scattered IR light. The Si wafer has been tested with a THz time-domain spectrometer, and its transmittance between 0.1–2.5 THz is $\sim 49\%$. This is compensated when calculating the extracted THz energies as well as the corresponding efficiencies.

It has been reported that with the TPF method, high optical-to-THz efficiency should be obtained with Fourier transform limited (FTL) laser pulses. For 800 nm pump wavelengths, the optimal FTL pulse duration is ~ 350 fs^[25]. Experiments based on the spectrum-cutting method has already verified it^[30,31]. In our case, we introduce the temporal chirp method to stretch the pump pulses. Figure 2(a) illustrates the extracted THz energies as a function of the second-order dispersion of the pump laser pulses. We optimized the TPF setup while fixing the pump laser energy at 10 mJ measured before the HWP between the grating and the lens. For different pump energies, the TPF setup needs to be optimized due to the nonlinear distortion effect. Adjusting the second-order dispersion, a maximum THz output energy of ~ 19.5 μJ is obtained at a second-order dispersion of 3000 fs^2 with corresponding positively chirped pulse

duration of 187 fs. With this optimal chirped pulse duration, we measured the output THz energy and its corresponding efficiency dependent on the pump laser energy, shown in Fig. 2(b). The THz energy increases with the pump energy following a quadratic behavior until 12 mJ. For this case, the maximum extracted THz energy is 40 μJ . The corresponding extracted THz efficiency increases linearly with the pump energy, and the maximum number is 0.16% in this case. However, further increasing the pump energy, the THz yields increases slowly, and the efficiency saturates and decreases. When the pump energy is scaled up to 31 mJ, the efficiency has already decreased to 0.13%. It is expected that the output THz energy will saturate very fast due to the decreasing behavior of the efficiency. This means higher THz energy cannot be obtained with simply scaling up the pump energy, even if we already stretch the pump pulse duration from 30 to 187 fs.

According to the nonlinear distortion effect^[32], the optimization condition of the TPF setup for different pump energies is different. Therefore, we fixed the pump pulse duration at 30 fs (TFL) and optimized the TPF setup at 20 and 30 mJ, respectively. Figure 3 shows the extracted THz energy and its corresponding efficiency

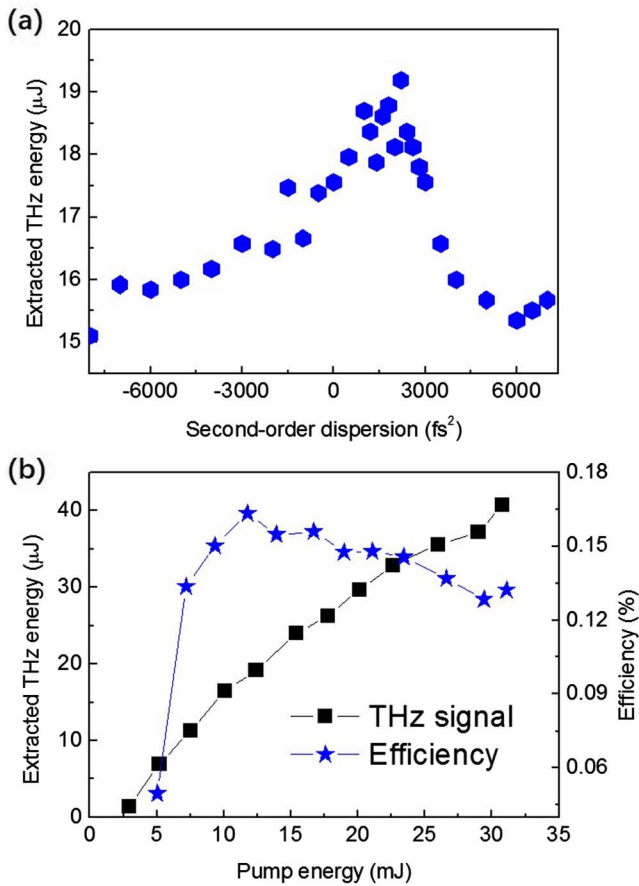


Fig. 2. (a) Extracted THz energy as a function of the second-order dispersion at 10 mJ pump energy. (b) Extracted THz energy and its corresponding optical-to-THz energy conversion efficiency for different pump energies at a chirped pulse duration of 187 fs.

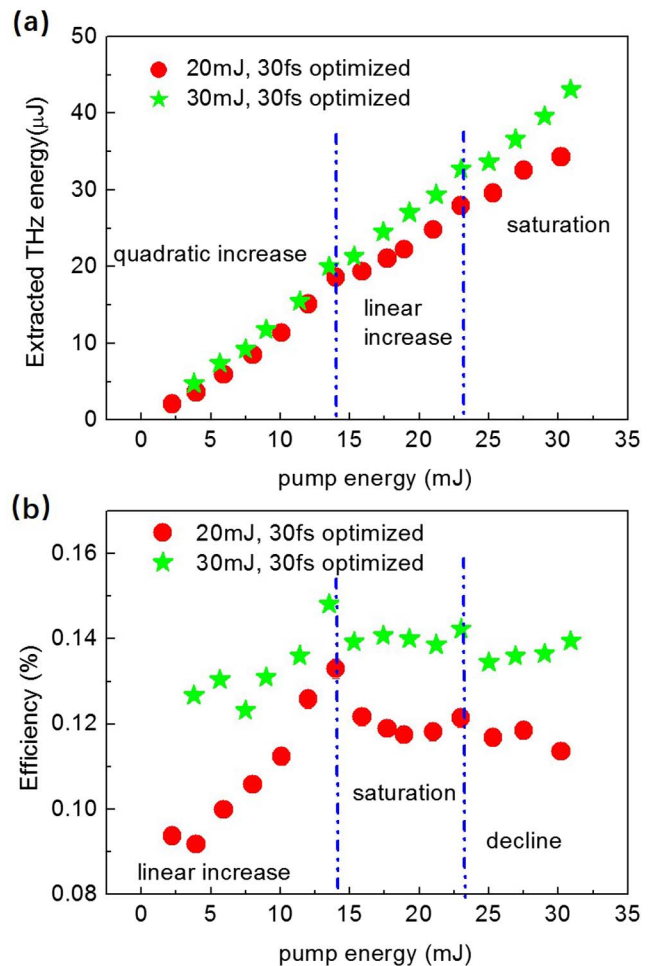


Fig. 3. (a) Extracted THz energy and (b) the corresponding optical-to-THz conversion efficiency depending on pump energy.

optimized at the above different pump energies. The THz energy curve obtained at 30 mJ, 30 fs pumping is slightly higher than that measured at 20 mJ, 30 fs pumping. As a consequence, the efficiency is enhanced by scaling up the optimization pump energy from 20 to 30 mJ. For both cases, when the pump energy is lower than 15 mJ, the THz energy increases with the pump energy in a quadratic way. Further increasing the pump energy to 23 mJ, the THz energy is enhanced linearly, while it starts to saturate when the pump energy is scaled up to 31 mJ. Both corresponding efficiency curves first linearly increase with the pump energy till 15 mJ and then saturate.

Although the efficiency obtained at the optimization of 30 mJ pump pulses is higher than that optimized at 20 mJ, the absolute efficiency is lower than that optimized at 10 mJ, 187 fs, which is compared in Fig. 4. The best efficiency for the three optimization conditions is achieved under the optimization parameters of 10 mJ, 187 fs. The maximum THz efficiency obtained at 10 mJ, 187 fs pumping is 0.17%, while it is only 0.15% for 30 mJ, 30 fs laser pulses, although the pump peak intensity of 30 mJ, 30 fs pumping is 20 times higher than that of 10 mJ, 187 fs. According to the second-order nonlinear effect of optical rectification, the THz efficiency should increase with the increasing pump peak intensity when ignoring the influence of the effective interaction length. The main reasons for the efficiency saturation are discussed below. The optical nonlinear down conversion cascading process in optical rectification implies higher optical-to-THz efficiency as long as the phase matching condition is satisfied^[33]. Longer pump pulse durations guarantee longer effective interaction lengths and consequently higher efficiencies^[25]. Furthermore, free-carrier generation due to multi-photon absorption in LN (band-gap: 4.0 eV) becomes more pronounced at shorter pulse pumping. The generated free-carriers absorbing THz photons inside LN result in lower out-coupled efficiency of the THz waves^[29]. The pump peak intensity, effective interaction length, and the multi-photon absorption

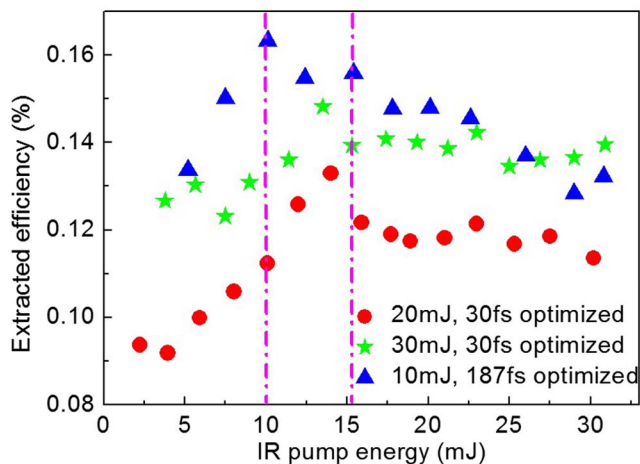


Fig. 4. Optical-to-THz energy conversion efficiency as a function of pump energy at different optimization parameters.

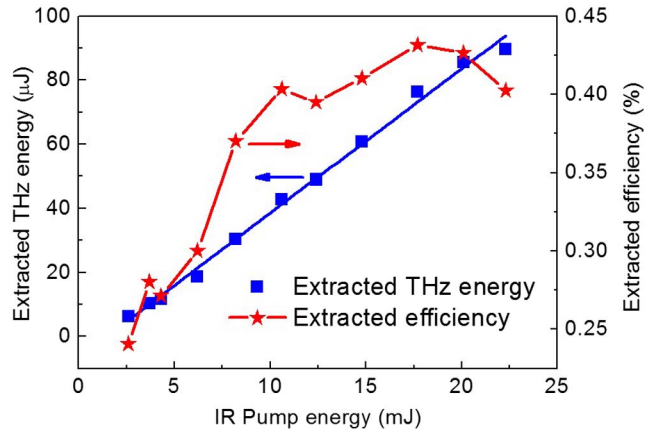


Fig. 5. Extracted THz energy and its corresponding efficiency as a function of the pump energy. The TFP setup was optimized at a fixed pump parameter of 10 mJ pump energy with 187 fs pulse duration, and the iris before the compressor was slightly closed.

compete in the cascading process for highly efficient THz generation. Our experimental results show that the effective interaction length and the multi-photon absorption dominate the competition.

With the above obtained optimal pulse duration of 187 fs, we optimized the TFP setup at 10 mJ, and then slightly closed the iris after the compressor of the pump laser system. An enhanced THz yield is obtained, as shown in Fig. 5. The extracted THz energy increases linearly with the pump energy. A maximum THz energy of 90 μ J and its corresponding optical-to-THz efficiency of 0.43% are achieved at the maximum pump energy of 21 mJ. A record efficiency of 0.43% is achieved in LN via optical rectification at room temperature driven by an 800 nm laser wavelength. For the triangle shape of the LN crystal, efficient THz generation happens close to the cutting edge of the phase matching angle in the x - y plane. In order to avoid damage to the crystal, the laser pump beam on the entry face of the LN crystal is ~ 20 mm in diameter ($1/e^2$). In this case, a large part of the pump laser beam does not contribute to THz generation, consequently resulting in lower efficiency. When slightly closing the iris before the laser compressor, we not only reduce the beam size of the pump laser pulses leading to higher peak intensity due to diffraction, but also eliminate the low energy portion, which was once considered in calculating the optical-to-THz efficiency.

To conclude this work, we systematically investigate the optimization conditions of TPF in LN pumped by Ti:sapphire laser pulses at an 800 nm wavelength with 30 fs TFL pulse duration. Compared with the pump energy, the pulse duration of the pump pulses plays a decisive role in scaling up the THz efficiency. A record efficiency of 0.43% is achieved in LN via optical rectification at room temperature driven by 800 nm laser pulses. Our approach provides a new method for the mJ THz generation with the TPF technique in LN excited by the existing J-level Ti:sapphire lasers, which deliver sub-50-fs pulse durations.

This work was supported by the National Basic Research Program of China (No. 2013CBA01501), the National Natural Science Foundation of China (No. 11520101003), and the Strategic Priority Research Program of the Chinese Academy of Sciences (Nos. XDB16010200 and XDB07030300). Dr. Xiaojun Wu thanks the “Zhuoyue” Program of Beihang University (No. GZ216S1711).

References

1. Y.-S. Lee, *Principles of Terahertz Science and Technology* (Springer, 2009).
2. M. Exter, C. Fattinger, and D. Grischkowsky, *Opt. Lett.* **14**, 1128 (1989).
3. Y. Yang, M. Mandehgar, and D. Grischkowsky, *Opt. Lett.* **20**, 26208 (2012).
4. R. I. Stantchev, D. B. Phillips, P. Hobson, S. M. Hornett, M. J. Padgett, and E. Hendry, *Optica* **4**, 989 (2017).
5. H. A. Hafez, X. Chai, A. Ibrahim, S. Mondal, D. Férachou, X. Ropagnol, and T. Ozaki, *J. Opt.* **18**, 093004 (2016).
6. D. Nicoletti and A. Cavalleri, *Adv. Opt. Photon.* **8**, 401 (2016).
7. P. K. Mishra, O. Vendrell, and R. Santra, *Angew. Chem. Int. Ed.* **52**, 13685 (2013).
8. V. I. Fedorov, *Biophysics* **62**, 324 (2017).
9. N. Stojanovic and M. Drescher, *J. Phy. At. Mol. Opt. Phys.* **46**, 192001 (2013).
10. X. Ropagnol, M. Khorasaninejad, M. Raeiszadeh, S. S. Naeini, M. Bouvier, C. Y. Côté, A. Laramée, M. Reid, M. A. Gauthier, and T. Ozaki, *Opt. Express* **24**, 11299 (2016).
11. N. T. Yardimci, S. H. Yang, C. W. Berry, and M. Jarrahi, *IEEE Trans. THz. Sci. Tech.* **5**, 223 (2015).
12. K. Y. Kim, A. J. Taylor, J. H. Glowina, and G. Rodriguez, *Nat. Photon.* **2**, 605 (2008).
13. C. Vicario, A. V. Ovchinnikov, S. I. Ashitkov, M. B. Agranat, V. E. Fortov, and C. P. Hauri, *Opt. Lett.* **39**, 6632 (2014).
14. W. R. Huang, A. Fallahi, X. Wu, H. Cankaya, A.-L. Calendron, K. Ravi, D. Zhang, E. A. Nanni, K. H. Hong, and F. X. Kärtner, *Optica* **3**, 1209 (2016).
15. X. Zhao, J. Zhang, K. Fan, G. Duan, G. D. Metcalfe, M. Wraback, X. Zhang, and R. D. Averitt, *Photon. Res.* **4**, A16 (2016).
16. C. Lange, T. Maag, M. Hohenleutner, S. Baierl, O. Schubert, E. R. J. Edwards, D. Bougeard, G. Woltersdorf, and R. Huber, *Phys. Rev. Lett.* **113**, 227401 (2014).
17. K. Iwaszczuk, M. Zalkovskij, A. C. Strikwerda, and P. U. Jepsen, *Optica* **2**, 116 (2015).
18. R. Matsunaga, N. Tsuji, H. Fujita, A. Sugioka, K. Makise, Y. Uzawa, H. Terai, Z. Wang, H. Aoki, and R. Shimano, *Science* **345**, 1145 (2014).
19. T. Kampfrath, K. Tanaka, and K. A. Nelson, *Nat. Photon.* **7**, 680 (2013).
20. J. Hebling, G. Almási, and I. Z. Kozma, *Opt. Express* **10**, 1161 (2002).
21. A. Yahaghi, K. Ravi, A. Fallahi, and F. Kärtner, *J. Opt. Soc. Am. B* **34**, 590 (2017).
22. M. I. Bakunov, S. B. Bodrov, and E. A. Mashkovich, *J. Opt. Soc. Am. B* **28**, 1724 (2011).
23. J. A. Fülöp, G. Polónyi, B. Monoszlai, G. Andriukaitis, T. Balciunas, A. Pugzlys, G. Arthur, A. Baltuska, and J. Hebling, *Optica* **3**, 1075 (2016).
24. K.-L. Yeh, M. C. Hoffmann, J. Hebling, and K. A. Nelson, *Appl. Phys. Lett.* **90**, 171121 (2007).
25. J. A. Fülöp, L. Pálfalvi, G. Almási, and J. Hebling, *Opt. Lett.* **18**, 12311 (2010).
26. S.-W. Huang, E. Granados, W. R. Huang, K.-H. Hong, L. E. Zapata, and F. X. Kärtner, *Opt. Lett.* **38**, 796 (2013).
27. J. A. Fülöp, Z. Ollmann, C. Lombosi, C. Skrobol, S. Klingebiel, L. Pálfalvi, F. Krausz, S. Karsch, and J. Hebling, *Opt. Lett.* **22**, 20155 (2014).
28. M. Kunitski, M. Richter, M. D. Thomson, A. Vredenburg, J. Wu, T. Jahnke, M. Schöffler, H. S.-B. Böcking, H. G. Roskos, and R. Dörner, *Opt. Express* **21**, 6826 (2013).
29. X. Wu, S. Carbajo, K. Ravi, F. Ahr, G. Cirmi, Y. Zhou, O. D. Mücke, and F. X. Kärtner, *Opt. Lett.* **39**, 5403 (2014).
30. F. Blanchard, X. Ropagnol, H. Hafez, H. Razavipour, M. Bolduc, R. Morandotti, T. Ozaki, and D. G. Cooke, *Opt. Lett.* **39**, 4333 (2014).
31. S.-C. Zhong, J. Li, Z.-H. Zhai, L.-G. Zhu, J. Li, P.-W. Zhou, J.-H. Zhao, and Z.-R. Li, *Opt. Express* **24**, 14828 (2016).
32. C. Lombosi, G. Polónyi, M. Mechler, Z. Ollmann, J. Hebling, and J. A. Fülöp, *New J. Phys.* **17**, 083041 (2015).
33. K. Ravi, W. R. Huang, S. Carbajo, X. Wu, and F. X. Kärtner, *Opt. Express* **22**, 20239 (2014).